iScience, Volume *23*

Supplemental Information

Skeletal-Muscle Metabolic Reprogramming in ALS-SOD1^{G93A} Mice Predates Disease Onset and Is A Promising Therapeutic Target

Silvia Scaricamazza, Illari Salvatori, Giacomo Giacovazzo, Jean Philippe Loeffler, Frederique Renè, Marco Rosina, Cyril Quessada, Daisy Proietti, Constantin Heil, Simona Rossi, Stefania Battistini, Fabio Giannini, Nila Volpi, Frederik J. Steyn, Shyuan T. Ngo, Elisabetta Ferraro, Luca Madaro, Roberto Coccurello, Cristiana Valle, and Alberto Ferri

Figure S1

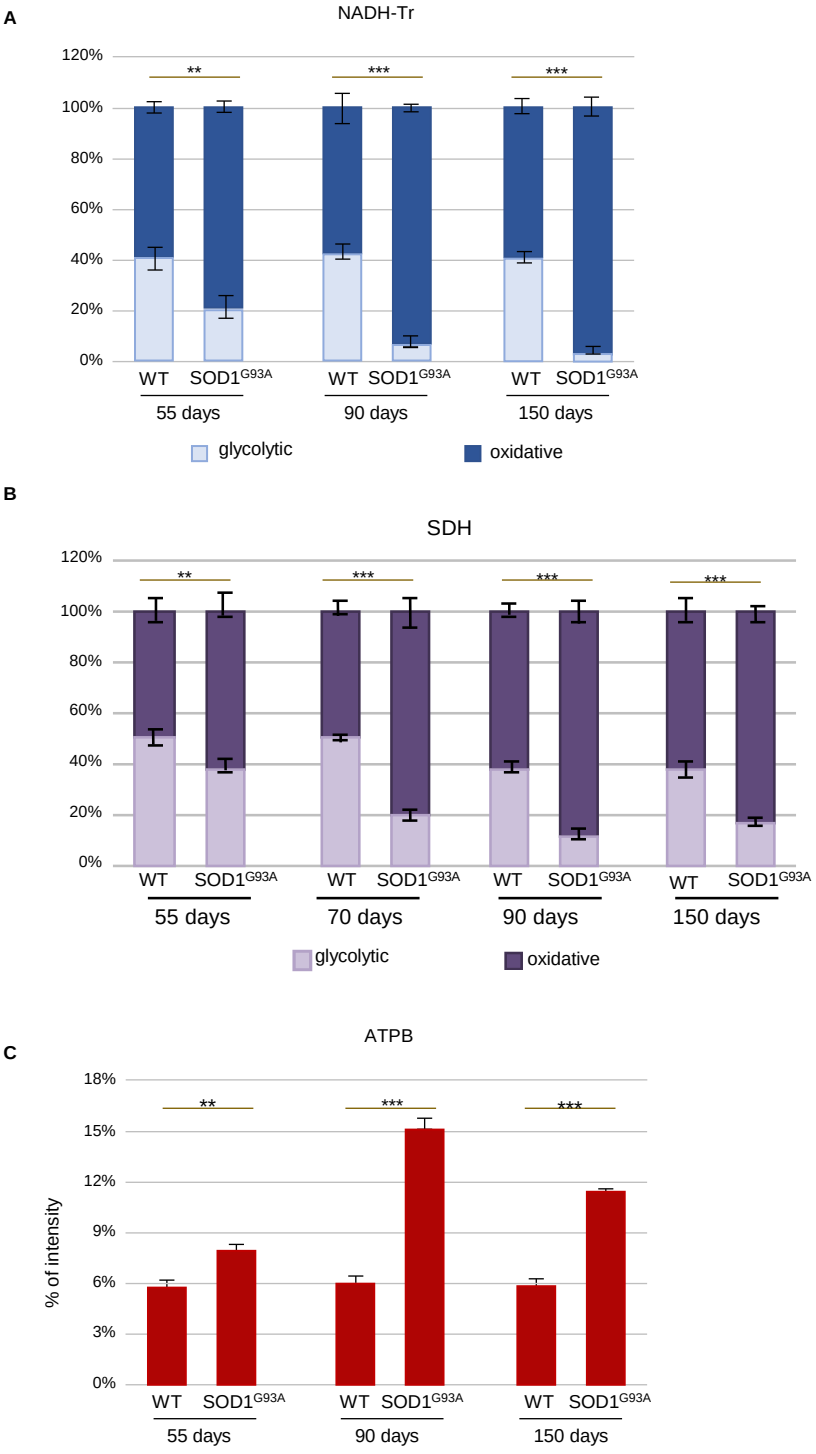

Figure S1. Quantification of muscle oxidative markers, Related to Figure 2. (A-B) Percentages of the dark areas (Blue for NADH-Tr activity and Purple for SDH activity, respectively) measured using ImageJ and normalized against total area. **(C)** Percentages of the red areas (ATBP fluorescent signal) measured using ImageJ and normalized against total area. Calculations were performed on tibialis anterior (TA) cryosections (3 for each mouse) from 3 to 4 different mice at each age. Data presented as means ± SEM, ***P*<0,001, ****P*<0,0001 with respect to wild-type control littermates at the same age, unpaired Student's *t* tes.

Figure S2

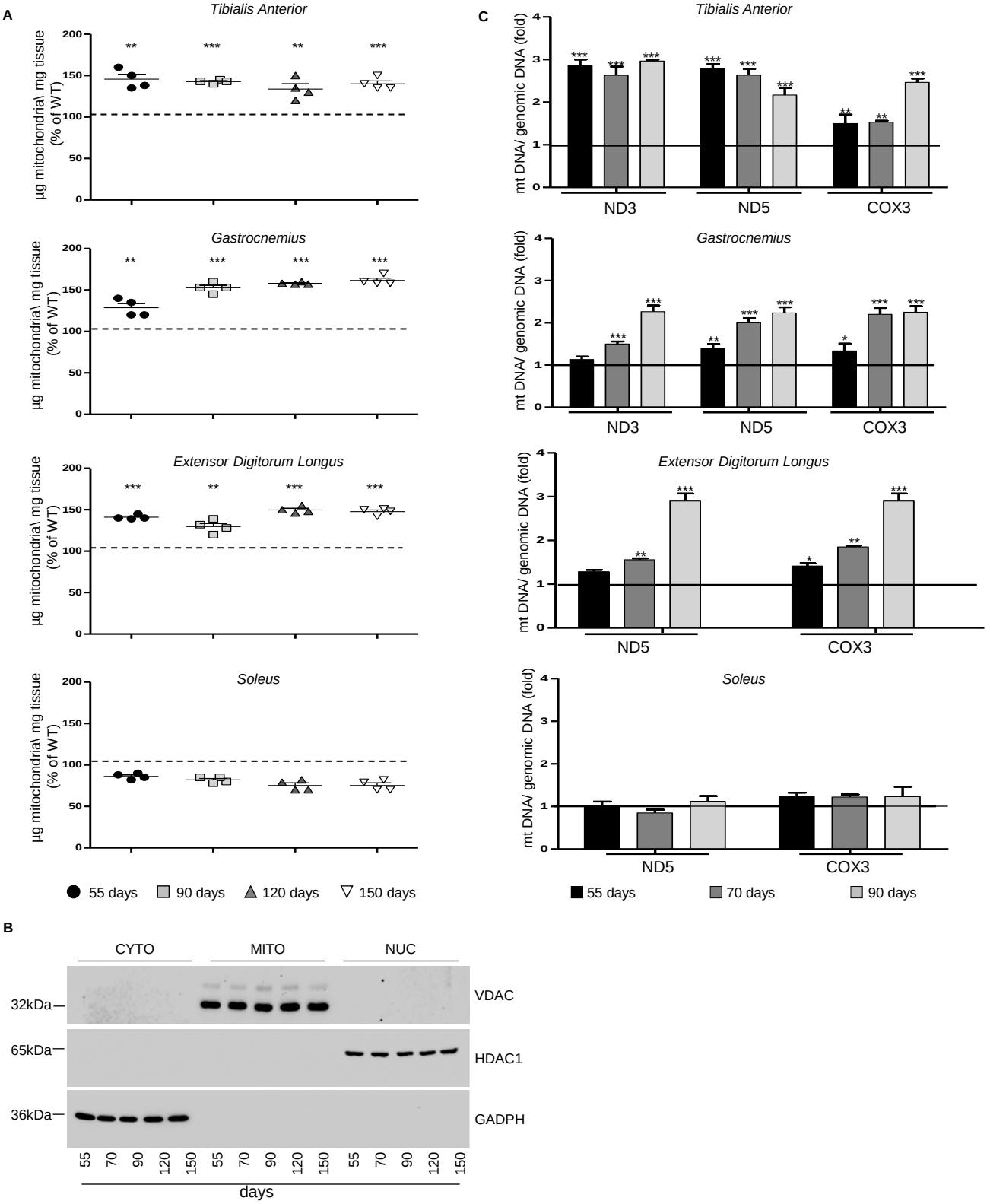

Figure S2. The mass of mitochondria increases during disease course, Related to Figure 2. Mitochondrial amount was determined at 55, 90, 120 and 150 days of age by assessing: **(A)** The ratio between ug of purified mitochondria and mg of tissue used for purification; *tibialis anterior* (TA), *gastrocnemius* (GNM), *extensor digitorum longus* (EDL) and *soleus.* Data are reported as percentage, with 100% being assigned to values obtained from age-matched wild-type control mice (WT), $n = 4$ independent experiments. **(B)** Western blot analysis of cytosolic (CYTO), mitochondrial (MITO) and nuclear (NUC) subcellular fractions obtained from the TA of WT mice from 55 to 150 days of age. Fractions were verified for the presence of specific markers using antibodies against GADPH for the cytosolic fraction, VDAC for the mitochondrial fraction and HDAC1 for the nuclear fraction. A representative immunoblot is shown. **(C)** RT-qPCR quantification of ND3, ND5 and COX3 genes encoded by mitochondrial DNA in the TA, GNM, EDL and soleus muscle. Genomic DNA was used as internal standard and values of age-matched wild-type control mice was arbitrary set at 1. Data are presented as mean ± SEM, *P<0,05, **P<0,001, ***P<0,0001, unpaired Student's t test, n=4 different mice for each age.

Figure S3

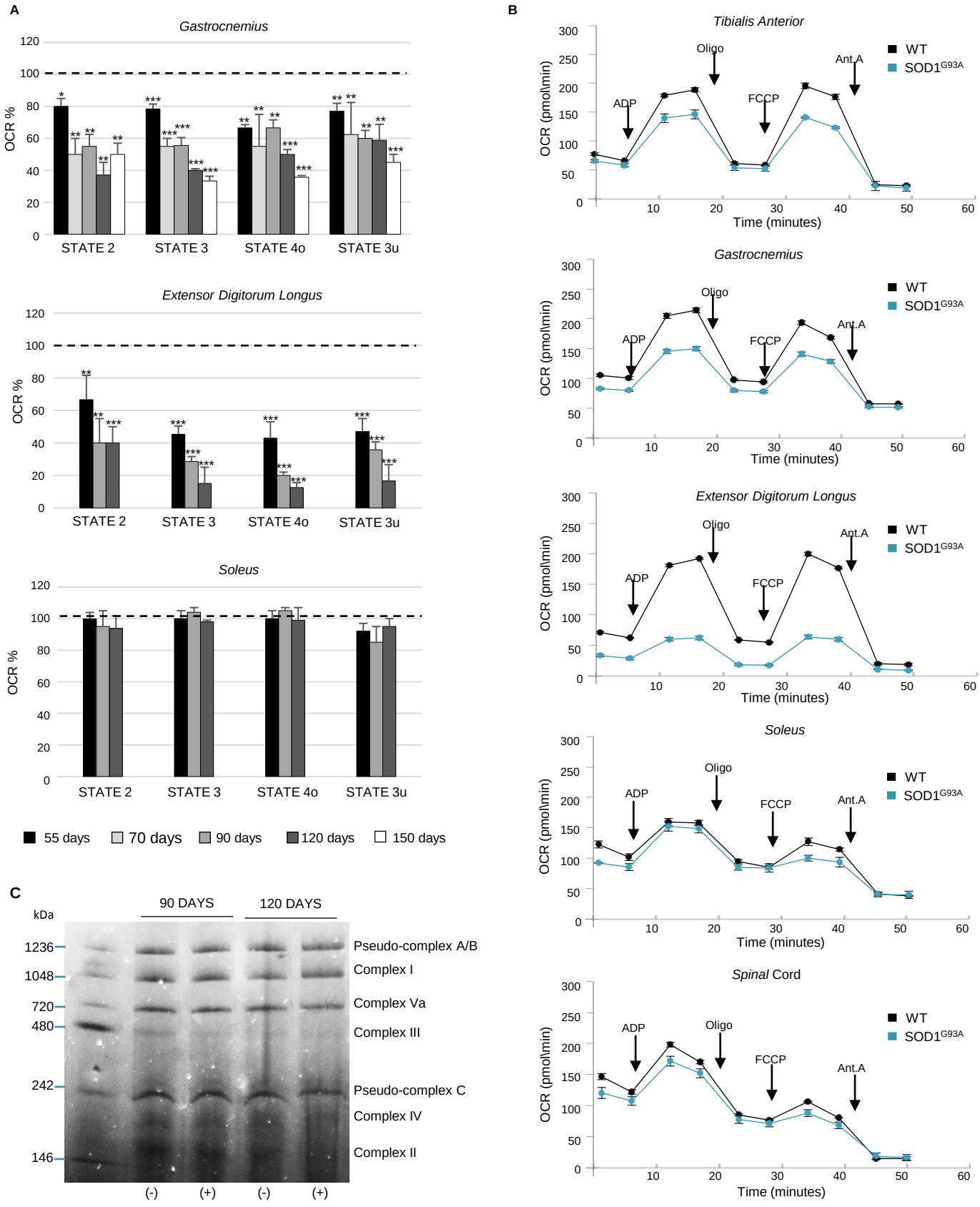

Figure S3. Mitochondrial bioenergetic failure occurs in skeletal muscle of early presymptomatic SOD1 G93A mice, Related to Figure 3. (A) Coupling assay on isolated mitochondria purified from different tissues of SOD1^{G93A} mice at the indicated ages. Mitochondrial respiration stages are reported: basal respiration (State 2), maximally coupled respiration (State 3), respiration due to proton leak (State 4o) and maximal uncoupled respiration (State 3u). Data are expressed as % of Oxygen Consumption Rate (OCR) and 100% was arbitrarily assigned to values obtained from age-matched wild-type mice. *P<0,05, **P<0,001, ***P<0,0001, unpaired Student's t test. **(B)** Representative Coupling Assay profiles performed on mitochondria isolated from the indicated tissues of 55 day old SOD1^{G93A}mice and their wild-type control littermates. The injection of ADP, Oligomycin, FCCP and Antimycin A (Ant. A) are indicated with arrows. **(C)** Blue Native Gel mitochondrial extracts isolated from the TA of WT (-) and SOD1^{G93A} (+) mice at the indicated ages. A representative gel is shown (n=3 experiments).

Figure S4

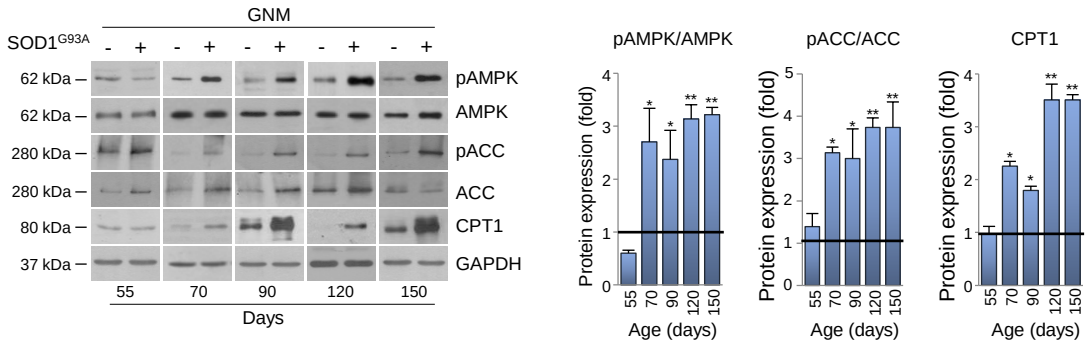

Figure S4. Alterations in metabolic targets occur early in the *gastrocnemius* of SOD1^{G93A} mice, Related to Figure 5. Western blot analysis of pAMPK, AMPK, pACC, ACC and CPT1 in the *gastrocnemius* (GMN) of SOD1^{G93A} (+) and wild type mice (-) from 55 days of age to end-stage (150 days) of disease. GAPDH was used as loading control (left panel). Densitometric analysis of pAMPK/AMPK and pACC/ACC ratios, and CPT1 expression (right panel). Data are presented as mean ± SEM, **P*<0,05, ***P*<0,001 when compared with wild-type mice at the same age (arbitrarily set at 1), *n* = 4 independent experiments, unpaired Student's *t* test.

Figure S5

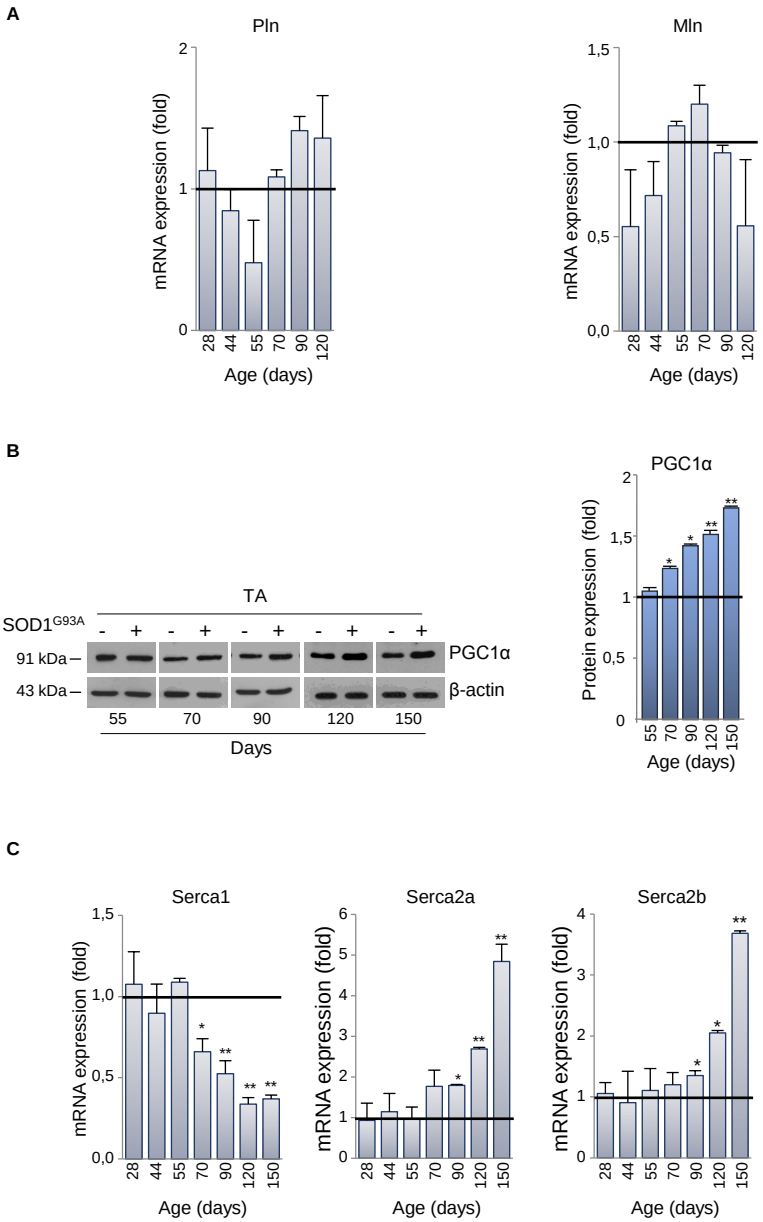

Figure S5. Expression of other SERCA regulating micropeptides, Related to Figure 6. (A) Expression of mRNAs coding for phospholamban (PLN) and myoregulin (MLN) in *tibialis anterior* of SOD1^{G93A} mice. RT-qPCR analysis was performed at different stages of disease in SOD1^{G93A} mice and their wild-type control littermates. **(B)** PGC1α expression in skeletal muscle of SOD1^{G93A} mice. PGC1α protein expression in *tibialis anterior* (TA) of SOD1^{G93A} (+) and wild type mice (-) at the indicated ages (left panel). β-Actin was used as loading control. Densitometric analysis of data (right panel), presented as mean ± SEM, **P*<0,05, ***P*<0,001, when compared with wild-type mice at the same age (arbitrarily set ~~on~~ at 1), *n* = 4 independent experiments, unpaired Student's *t* test. **(C)** Expression of mRNAs coding for Serca1, Serca2a, Serca2b in the TA of SOD1^{G93A} mice. RT-qPCR analysis was performed at different stages of disease in SOD1^{G93A} mice and their wild-type control littermates (at least *n*=3 for each stage). Results in **A** and **C** (at least *n*=3 for each stage) are expressed as the ratio between the average of values from wild-type control and transgenic mice, normalized to the average values of TATA box housekeeping gene. Data are presented as mean ± SEM when compared with control littermates at the same age (arbitrarily set ~~on~~ at 1), unpaired Student's *t* test.

Figure S6

A

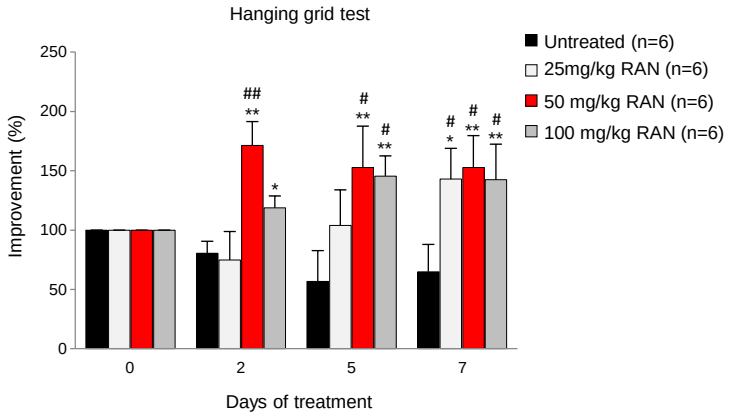

B

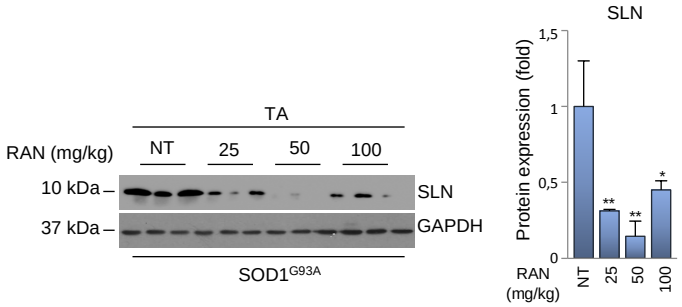

Figure S6. Dose response study of Ranolazine treatment, Related to Figure 7. (A) Locomotor abilities of SOD1^{G93A} mice receiving daily intraperitoneal injection of different doses of Ranolazine (RAN) (25, 50 and 100 mg/kg) or physiological solution (untreated) for seven days (from 110 to 117 days of age) evaluated by hanging grid test at the indicated days. Performance at day 0 of treatment was considered as 100% and performance, at days 2, 5 and 7, were considered relative to time 0. *P<0,05, **P<0,001 when compared with untreated SOD1^{G93A} and $^{\#}P$<0,05, $^{\#\#}P$<0,001 when compared with SOD1^{G93A} performance at the beginning of treatment. **(B)** Western blot analysis of Sarcolipin (SLN) in the *tibialis anterior* (TA) of SOD1^{G93A} receiving daily intraperitoneal injection of RAN 25 mg/kg (25), 50 mg/kg (50), 100 mg/kg (100) or physiological solution (NT) for seven days (left panel). GAPDH antibody was used as loading control. Densitometric analysis of data (right panel). *P<0,05, **P<0,001 when compared with untreated mice (arbitrarily set at 1). Data are presented as mean ± SEM of $n = 6$ independent experiments, parametric two-way ANOVA with Bonferroni *post hoc* test (A) and one-way ANOVA with Bonferroni *post hoc* test (A).

Figure S7

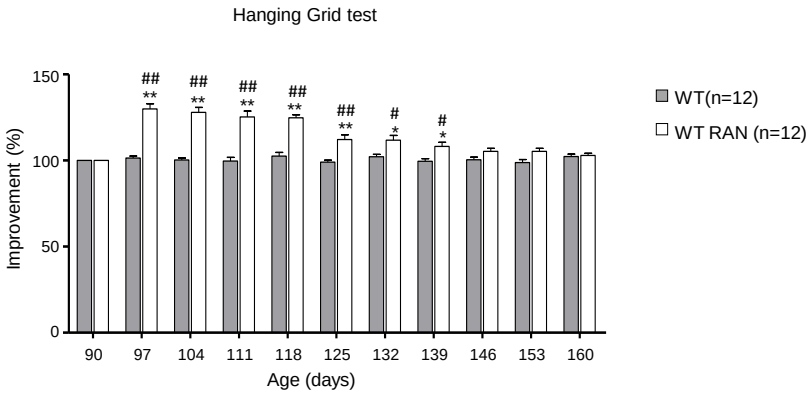

Figure S7. Ranolazine (RAN) treatment effect in wild-type (WT) mice, Related to Figure 7. Locomotor abilities of WT mice receiving daily intraperitoneal injection of Ranolazine 50 mg/kg (WT RAN) or physiological solution (WT) evaluated by hanging grid test at the indicated days. Performance was evaluated from 90 days of age (start of treatment) to an age that equates to the end-stage of disease for $SOD1^{G93A}$ mice. Data are presented as mean ± SEM, **P*<0,05 ***P*<0,001 when compared with age-matched WT untreated mice and $^{\#}P$<0,05 $^{\#\#}P$<0,01 when compared with WT mice at the beginning of treatment, *n*=11 WT, *n* = 11 WT RAN, parametric two-way ANOVA with Bonferroni *post hoc* test.

METHODS

Antibodies

The antibodies used in this study were: AMPKα rabbit polyclonal (Cell Signaling, Cat#2532 WB:1:1000), Phospho-AMPKα (Thr172) (40H9) rabbit monoclonal (Cell Signaling, Cat#2535 WB:1:1000), Acetyl-CoA Carboxylase (c83b10) rabbit monoclonal (Cell Signaling, Cat#3676 WB:1:1000), Phospho-Acetyl-CoA Carboxylase (Ser79) rabbit polyclonal (Cell Signaling, Cat#3661 WB:1:1000), anti-CPT1A (8F6AE9) mouse monoclonal (Abcam 128568 WB:1:1000), anti-Sarcolipin rabbit polyclonal (Millipore Cat#ABT13 WB 1:1000), CaMKIIα (A-1) mouse monoclonal (Santa Cruz Biotechnology Inc,. Cat# sc-13141 WB 1:1000), Phospho-CaMKIIα (22B1) mouse monoclonal (Santa Cruz Biotechnology Inc., Cat# sc-32289 WB 1:1000), PGC1alpha (H-300) Rabbit polyclonal (Santa Cruz Biotechnology Inc., Cat# sc-13067 WB 1:1000), anti-Laminin rabbit polyclonal (Cat#L9393, Sigma, IF 1:400), Anti- ATPB (3D5) mouse monoclonal (Abcam Cat#ab14730 IF 1:400), anti-HDAC1 rabbit polyclonal (Santa Cruz Biotechnology Inc., Cat# sc-7872, RRID:AB_2279709, WB 1 : 1000), anti-VDAC mouse monoclonal (Santa Cruz Biotechnology Inc., Cat# sc-8829, RRID:AB_2214801, WB 1 : 5000), anti-GAPDH mouse monoclonal (Santa Cruz Biotechnology Inc., Cat# sc-166545, RRID:AB_2107299 WB 1:5000), anti-β-Actin (Santa Cruz Biotechnology Inc., Cat# sc-47778, WB 1:5000). Anti-rabbit (Cat# 1706515, WB: 1:1000) and anti-mouse (Cat# 1706516, WB: 1:1000) IgG peroxidase-conjugated secondary antibodies were from Bio-Rad Laboratories, Hercules, CA, USA and Alexa Fluor 488 (Invitrogen, Cat# A11017, 1: 300) anti-rabbit goat antibodies and Cy3 anti-mouse antibody from Jackson Immuno-Research Laboratories, West Grove, PA, USA, Cat# 65119, 1: 300).

Animals

All animal procedures were carried out in accordance with the European Guidelines for the use of animals in research (2010/63/EU) and the requirements of Italian laws (D.L. 26/2014). All procedures were approved by the Animal welfare office, Department of Public Health and Veterinary, Nutrition and Food Safety, General Management of Animal Care and Veterinary Drugs of the Italian Ministry of Health (protocol number 931/2017/PR). Animals were kept in a virus/antigen-free facility with a light/dark cycle of 12 h at constant temperature and humidity. Food and water were provided *ad libitum*.

SOD1^{G93A} mice (B6.Cg-Tg(SOD1 G93A)1Gur/J) were obtained from The Jackson Laboratory (Bar Harbor, ME, USA) and bred in our animal facility. Transgenic hemizygous SOD1^{G93A} males were crossbred with C57BL/6 females and transgenic progeny were genotyped by PCR. Disease onset was evaluated by hanging grid test; tests were conducted once per week starting at 55 days of age. The final measurement for each mouse was determined by calculating the mean of three different hanging grid test trials on each given day. A performance baseline of 100% was assigned to the first mean performance for each mouse at 55 days of age. Age of symptom onset was classified as being the time at which mouse performance deteriorated by 20% from the baseline. In our animal house, and using this approach, disease onset in male mice was classified as being 91.7 ± 2.9 days, and survival was 168.7 ± 1.9 days.

To follow disease progression, behavioural scores and body weight were monitored starting at 55 days according to Apolloni et al. (Apolloni et al., 2019). In brief, we assigned the following age (in days) to the following disease stages: 55 days as “early presymptomatic”, 70 days as “presymptomatic”, 90 days as “symptoms onset”, 120 days as “symptomatic”, 150 days as “end stage”. Mice were anaesthetized with Rompum (xylazine, 20 mg/ml, 0.5 ml/kg Bayer, Milan, Italy) plus Zoletil (tiletamine and zolazepam, 100 mg/ml, 0.5 ml/kg; Virbac, Milan, Italy), and then sacrificed for tissue dissection.

Energy metabolism by indirect calorimetry

Total Energy Expenditure (EE), Resting Energy Expenditure (REE) and Respiratory Exchange Ratio (RER) were measured using an indirect calorimeter system (TSE PhenoMaster/LabMaster System, Germany) with a constant air flow of 0.35 L/min. Mice were adapted for 12 hours to the metabolic chamber, and parameters were measured at 20 minute intervals for each mouse, starting at 7:00 PM and ending automatically after 48h or 72h (12h dark-light phase comparison). Room temperature was kept constant (22˚±1˚C) and locomotor activity was assessed in parallel to discriminate between EE and REE. REE was analyzed by considering each animal's resting conditions, which was defined as an activity count between 0 and 3. RER was calculated as: RER = volume of CO_2 produced/volume of O_2 consumed (an index of substrate utilization). Mice were assessed under standard nutritional conditions (i.e., standard diet-fed) and food intake was continuously monitored (Giacovazzo et al., 2018)**.**

Glucose tolerance test (GTT)

GTT was performed in SOD1^{G93A} and WT mice at 55 days, 90 days and 120 days of age. Blood glucose was measured in tail tip blood samples using a Multicare Test Strip apparatus (Biochemical Systems International, Italy). Plasma glucose was assessed at 0, 20', 40' and 60 min after i.p. glucose administration (2gr/kg), which was administered following an overnight fast (16h). The area under the curve was calculated using the trapezoidal rule.

RNAseq

Total RNA from the *tibialis anterior* (TA) muscles of 90 day old SOD1^{G93A} mice and their wild-type control littermates was extracted using TRI Reagent (Sigma) following the manufacturer's protocol. RNA was shipped to the sequencing IGA of Udine (https://appliedgenomics.org/it/). The libraries for sequencing were prepared using NuGEN Ovation System V2 RNA–Seq. For each biological sample two independent experiments were carried out for the isolation of RNA.

Read quality control was asserted through FastQC (https://www.bioinformatics.babraham.ac.uk/projects/fastqc/), and quality/adapter trimming was carried out using Trim Galore (https://www.bioinformatics.babraham.ac.uk/projects/trim_galore/), which itself is a wrapper for cutadapt. Subsequently, reads were pseudo aligned to transcriptome GRCm38 (mm10) using Kallisto version 0.43.1. Count tables were generated in R using the package tximport together with DESeq2. Differential expression of genes was conducted using DESeq2 with default options. Genes were considered differentially expressed if the adjusted *P*-value was<0.05.

RNA-seq data of this study have been deposited in the Sequence Read Archive (SRA) under the accession code: PRJNA623256 (https://www.ncbi.nlm.nih.gov/Traces/study/?acc=PRJNA623256)

Histochemistry and Immunofluorescence

For histochemistry and immunofluorescence analysis, 10 µm muscle cryosections were obtained from SOD1^{G93A} mice and their wild-type control littermates at different stages of the disease.

For NADH-tetrazolium reductase activity staining (NADH-TR), muscle cryosections were incubated for 15 min with a solution containing NADH and nitrotetra-zolium blue (# N8129 and #N6876, Sigma-Aldrich) in Tris-HCl (pH 7.4) at 37°C (Madaro et al., 2013). Enzymatic staining for succinate dehydrogenase (SDH) activity was performed according to Molinari et al. (Molinari et al., 2017). Briefly, TA cross-sections were incubated for 20′ at 37 °C in PBS containing 1 mg/ml of nitrotetrazolium blue chloride (Sigma-Aldrich, St. Louis, MO, USA) and 27 mg/ml of Na-succinate. After staining, sections were fixed with 4% PFA and images from three serial sections per animal were acquired using an Olympus BX53 (Olympus). Images were processed using Image analysis IAS software (Delta Sistemi).

For immunofluorescence, cryosections were fixed in 4% PFA for 10 min, permeabilized with 0.25% Triton for 15 min at room temperature, and blocked for 1 h with a solution containing 4% BSA in PBS. Samples were then incubated for 2 h at room temperature with primary antibodies followed by Alexa 488- or Cy5- conjugated secondary antibodies. After rinsing in PBS, cryosections were counterstained with 1 *μ*g/ml Hoechst 33342 (Sigma-Aldrich) in PBS and visualized with a Zeiss LSM 800 Confocal Laser Scanning Microscope. Fluorescence images were processed using ZEN 2.6 (Blue Edition) (Carl Zeiss, Milan, Italy) and Adobe Photoshop software (Adobe, San Jose, CA, USA). Densitometric analyses were performed using ImageJ (U. S. National Institutes of Health, Bethesda, Maryland, USA, https://imagej.nih.gov/ij/, 1997-2016).

Isolation, quantification and bioenergetic analysis of isolated mitochondria

Mitochondria were isolated from the TA, gastrocnemius (GNM), extensor digitorum longus (EDL), soleus and spinal cord of $SOD1^{G93A}$ mice and their wild-type control littermates, at different stages of the disease. According to Salvatori et al., tissues were homogenized in 210 mM mannitol, 70 mM sucrose, 1 mM EDTA and 10 mM HEPES KOH (pH 7.5) through a Glass/Teflon Potter Elvehjem homogenizer (Salvatori et al., 2017, 2018). The total concentration of mitochondria was determined using a Bradford assay (Bio-Rad, Cat# 5000006) and the obtained quantity was normalized to the weight of the starting material to determine μg of mitochondria per mg of tissue. Tissue mitochondrial content was also assayed by quantitative real-time PCR in which the quantity of mitochondrial DNA / genomic DNA was evaluated (see also below in “DNA-RNA isolation and Real Time PCR”).

Isolated mitochondria were resuspended in a minimum volume of Respiration Buffer (250 mM Sucrose, 15 mM KCl, 1 mM EGTA, 5 mM $MgCl_2$, 30 mM K_2HPO_4), loaded (4 μg for skeletal muscles and 12 μg for spinal cord) onto a Seahorse XFe96 microplate, and centrifuged for 20 minutes at 2000 x g. After centrifugation 180 μl of Respiration Buffer [containing substrates: pyruvate (5 mM), malate (2.5 mM), glutamate (5 mM)] were added to each well, and the microplate was incubated at 37°C for 8 min to equilibrate the plate temperature. During plate incubation, the XFe96 cartridge was loaded with drugs to a final concentration of: ADP 1 mM, oligomycin 3 μM , FCCP 12 μM and Antimycin A 2 μM. Microplates containing mitochondria were then loaded into Seahorse XFe96 Extracellular Flux Analyzer (Seahorse Bioscience-Agilent) and the assay was completed according to the protocol developed by Seahorse Agilent. Coupling assays were performed across 6 technical replicates per plate, for 3 experiments. This assay allows for the assessment of electron transport chain functionality and oxidative phosphorylation flow tracing O_2 Consumption Rates (OCR) in basal conditions (mitochondrial State 2 respiration) and in response to the administration of ADP (maximal coupled respiration, or mitochondrial State 3 respiration), Oligomycin A (respiration due to proton leak, or mitochondrial State 4o

respiration), FCCP (maximal uncoupled respiration, or mitochondrial State 3u respiration) and Antimycin A (inhibition of oxidative respiration).

Blue Native PAGE (BN-PAGE)
BN-PAGE was performed on mitochondria purified from the TA of SOD1^{G93A} mice and their wild-type control littermates using a NativePAGE™ Sample Prep Kit (Invitrogen™, Cat # BN2008). Specifically, 20ug of mitochondrial protein was loaded into 4-16% gradient gels (Bio-Rad), electrophoresed at 150 V for 120 minutes, and stained with 10% acetic acid, 25% isopropanol and Coomassie blue G250. The apparent molecular weight was determined using NativeMark™ Unstained Protein Standard molecular weight markers (Invitrogen™, Cat # LC0725).

Total ATP evaluation
Total ATP concentration was measured in the TA of SOD1^{G93A} mice and their wild-type control littermates using an ATP Colorimetric/Fluorometric Assay Kit (BioVision, Inc., Milpitas, CA). Samples were loaded in 96-well microtiter plates and the fluorometric measurement of tissue ATP concentration was determined at Ex / Em = 535/587 nm using a plate reader (Perkin Elmer 1420 Multilabel Counter Victor3V).

Biochemical assays
The activity of respiratory chain complexes (Complex I, II/III, IV) was evaluated in isolated mitochondria obtained from ALS mice and their wild-type control littermates at different stages of the disease according to Salvatori et al. (Salvatori et al., 2018), with some modifications. Briefly, tissues were sonicated (UP200S Ultrasound Technology, Hielscher, Teltow, Germany, 20% Amplitude, 0.5 cycles for 30 s) and the reduction or oxidation of specific substrates was recorded by spectrophotometric measures. Complex I activity was performed by monitoring the oxidation of NADH at 340 nm at 30°C in a 1 mL quartz cuvette containing 25 mM potassium phosphate pH 7.4, 5 mM $MgCl_2$, 5 mg/mL bovine serum albumin, 1 mg/mL Antimycin A, 65 µM decylubiquinone, 130 µM NADH and 80 µg of total mitochondrial protein. Complex II/III activity was performed by monitoring the reduction of ferricytochrome c at 540 nm in a 1-ml cuvette at 30°C containing 20mM succinate, 0.5 mM EDTA, 2 mM KCN, and 25 µg total mitochondria protein. Complex IV activity was assayed following the oxidation of ferricytochrome c at 540 nm in a 1 ml cuvette at 30°C. Spectrophotometric determination of citrate synthase activity was measured according to Ferri et al. (Ferri et al., 2006) and values were used as standard internal controls.

Bioenergetic analysis of isolated skeletal muscle satellite cells
Skeletal muscle satellite cells were isolated from 55 day old SOD1^{G93A} mice and age-matched wild-type controls through magnetic beads-associated cells sorting according to Reggio et al. (Reggio et al., 2020). Mice were euthanized via cervical dislocation, and hindlimbs were carefully skinned, dissected and placed in HBSS supplemented with 2% BSA and 1% Pen/Strep (SupHBSS). Muscles were dissociated from bones in a sterile hood and minced into small pieces. Minced tissue was separated at 700 x g for 10 min at 4°C and digested with 2 µg/µl collagenase A (Roche), 2.4 U/ml dispase II (Roche), and 10 µg/ml DNase I (Roche) in DPBS w/calcium and magnesium, for 1h under agitation in a water bath at 37°C. Digested tissue was separated at 700 x g for 10 min at 4°C, resuspended in SupHBSS and sequentially filtered through 100 µm, 70 µm and 40 µm nylon cell strainers previously hydrated with SupHBSS. After each filtration step, the cell suspension was separated and resuspended. Red blood cells were lysed with RBC buffer (ChemCruz) between the 70 µm and 40 µm filtration steps by incubating the cell pellet in 1

ml of 1X RBC for 2.5 min on ice, and inactivated with SupHBSS. The final cell suspension was separated and resuspended in magnetic beads buffer (MBB) consisting of DPBS w/o calcium and magnesium supplemented with 0.5% BSA and 2 mM EDTA, and filtered through 30 µm cell strainer. Cell sorting was carried out by incubating the cell pellet with anti-CD45 and anti-CD31 antibody to eliminate immune/hematopoietic and endothelial cells. Incubation with anti-7-integrin antibody yielded the satellite cell fraction. To precipitate contaminating fibroblasts, the 7-integrin positive fraction was pre-plated for 2h in growth medium consisting of DMEM high-glucose Glutamax (Gibco), supplemented with 1 mM sodium pyruvate, 1% pen/strep, 20% FBS, 10% horse serum, and 2% chicken embryo extract. Unattached cells were recovered and plated for proliferation in CytoGROW medium (Resnova) at a density of 200000 cells/100 mm dish. After 4 days of proliferation, cells were trypsinized and counted for analysis using a Seahorse XFe96 Extracellular Flux Analyser (Seahorse Bioscience-Agilent, USA). Bioenergetic profiles of skeletal muscle satellite cells isolated from $SOD1^{G93A}$ mice and wild-type age-matched controls were performed using a Mito Stress Test Kit (Seahorse Bioscience), following the manufacturer's instructions and according to Salvatori and collaborators (Salvatori et al., 2018).

Human samples and ethics statement

Muscle biopsies from ALS patients were obtained for diagnostic purposes in the Department of Medical, Surgical and Neurological Sciences of the University of Siena, Siena, Italy. All patients signed informed consent to permit the use of their samples for research. Our study complies with the ethical standards established in the 1964 Declaration of Helsinki and its later amendments.

Electrophoresis and western blotting

Protein samples were separated by SDS–polyacrylamide gel electrophoresis and transferred to nitrocellulose membranes (Perkin Elmer, Cat# NBA085B). Membranes were blocked for 1 h in Tris-buffered saline solution with 0.1% Tween-20 (TBS-T) containing 5% BSA, and then incubated for 2 h at room temperature or overnight at 4°C with indicated primary antibodies, diluted in TBS-T containing 2% BSA. After rinsing with TBS-T solution, membranes were incubated for 1 h with the appropriate peroxidase-conjugated secondary antibody diluted in TBS-T containing 1% BSA, then washed and developed using the enhanced chemiluminescence detection system (Roche Molecular Diagnostics, CA, USA, Cat# n11500694001 or BIO-RAD Clarity™ Western ECL substrate Cat# 170-5061). Densitometric analyses were performed using ImageJ (U. S. National Institutes of Health, Bethesda, Maryland, USA, https://imagej.nih.gov/ij/, 1997-2016). Protein relative expression values were normalized to GAPDH or β-Actin. The apparent molecular weight of proteins was determined by calibrating the blots with pre-stained molecular weight markers (Bio-Rad Laboratories, Cat# 161-0394).

DNA-RNA isolation and Real Time qPCR

Mitochondrial and genomic DNA were isolated according to Miller (Miller, 2003), whereas total RNA was extracted with Trizol and retro-transcribed with a SensiFASTtm cDNA synthesis kit (Bioline Cat# BIO-65054). Mitochondrial DNA content and mRNA expression levels were determined by Real Time qPCR reactions using a Light Cycler 480 SYBR Green System (Roche ETC). Cp values were calculated using the 'second derivative max' algorithm of the Lightcycler software. Relative mitochondrial DNA content was normalized to the genomic genes TNF-alfa and Interleukin 2 (IL2), whereas mRNA relative expression values were normalized to the housekeeping gene TATA box binding protein. Results, where not specifically expressed, were reported as the ratio between the average of

values from wild-type control mice and SOD1^{G93A} mice, normalized to the average values of genomic genes or the housekeeping gene. Primers sequences are listed in Table 3.

Treatment and assessment of motor function

In order to evaluate the best effective dose of drug, 110 day old SOD1^{G93A} transgenic mice and their wild-type control littermates (n=6 for each dose) were treated for seven days with or without Ranolazine (Selleckchem, catalog #S1425) (0 mg/kg, 25 mg/kg, 50 mg/kg, 100 mg/kg) by daily intraperitoneal injection. Motor ability were monitored as described in Ferraro et al., and in detail elaborated here, using the hanging grid test at days 0, 2, 5 and 7 of treatment; the average value from three trials (recorded from each mouse) was averaged to determine the final test score (Ferraro et al., 2016). Improvements in performance was expressed as a percentage of the starting value obtained at day 0, which was designated as 100%. After seven days of treatment, animals were euthanized by cervical dislocation and the TA and GNM muscles were rapidly excised for subsequent analyses.

The selected dose of Ranolazine (50 mg/kg) was then administered to SOD1^{G93A} transgenic mice at the onset of the disease (90 days old) and wild-type age-matched control mice. A control group of SOD1^{G93A} transgenic and wild-type age-matched control mice were treated with physiological solution. Mice were weighed and assessed by the hanging grid test once per week starting at beginning of treatment. The final weekly hanging grid score per mouse per week was determined as above. Groups of 120 day (n=12) and 150 day old mice (n=11/12) were sacrificed for evaluation of mid- and long-term treatment effects respectively. Survival was determined by noting the day at which animals achieved full paralysis of hind limbs and were not able to right within 30 s after being turned on the back. At this stage animals were sacrificed according to guidelines for preclinical testing (Poppe et al., 2014). In order to minimize sex related differences, we used male mice for both pilot and long-term treatments.

HPLC analysis of plasma ranolazine concentration

Plasma (100 ul) obtained from treated and untreated mice was added to 200 ul of acetonitrile, vortexed, and kept on ice for 5 min. The samples were then centrifuged for 10 min at 19000 RCF at room temperature, and the supernatants were subsequently diluted in solvent A (0,3% H_3PO_4) at a 1:1 (v:v) ration. 20 ul of each sample was injected into a HPLC system (series 200, Perkin Elmer) equipped with a Supelcosil LC-318 column (5um particle size, 25 cmx4.6mm). The isocratic HPLC elution mobile phase was composed of solvent A and solvent B (35% acetonitrile, 0,3% H_3PO_4) 10:90 (v:v). The flow rate was 0.8 ml/min and the column was maintained at room temperature. Total run time was 31 min and the retention time of ranolazine was 15.75 min. The UV/Vis detector was set at a wavelength of 223 nm.

Data analysis

Data are presented as mean ± SEM. Data were analysed using Kaplan-Meier, Student's t-test (two group comparison), one-way or two-way ANOVA. Post-hoc analysis was carried out using Bonferroni or Tukey tests. Statistical analysis was carried out using Graphpad Prism 5 software.

REFERENCES

Apolloni, S., Caputi, F., Pignataro, A., Amadio, S., Fabbrizio, P., Ammassari-Teule, M., and Volonté, C. (2019). Histamine Is an Inducer of the Heat Shock Response in SOD1-G93A Models of ALS. Int. J. Mol. Sci. 20.

Ferraro, E., Pin, F., Gorini, S., Pontecorvo, L., Ferri, A., Mollace, V., Costelli, P., and Rosano, G. (2016). Improvement of skeletal muscle performance in ageing by the metabolic modulator Trimetazidine. J. Cachexia. Sarcopenia Muscle 7, 449–457.
Ferri, A., Cozzolino, M., Crosio, C., Nencini, M., Casciati, A., Gralla, E.B., Rotilio, G., Valentine, J.S., and Carri, M.T. (2006). Familial ALS-superoxide dismutases associate with mitochondria and shift their redox potentials. Proc. Natl. Acad. Sci. U. S. A. 103, 13860–13865.
Giacovazzo, G., Apolloni, S., and Coccurello, R. (2018). Loss of P2X7 receptor function dampens whole body energy expenditure and fatty acid oxidation. Purinergic Signal. 14, 299–305.
Madaro, L., Marrocco, V., Carnio, S., Sandri, M., and Bouché, M. (2013). Intracellular signaling in ER stress-induced autophagy in skeletal muscle cells. FASEB J. 27, 1990–2000.
Miller, F.J. (2003). Precise determination of mitochondrial DNA copy number in human skeletal and cardiac muscle by a PCR-based assay: lack of change of copy number with age. Nucleic Acids Res. 31, 61e – 61.
Molinari, F., Pin, F., Gorini, S., Chiandotto, S., Pontecorvo, L., Penna, F., Rizzuto, E., Pisu, S., Musarò, A., Costelli, P., et al. (2017). The mitochondrial metabolic reprogramming agent trimetazidine as an 'exercise mimetic' in cachectic C26-bearing mice. J. Cachexia. Sarcopenia Muscle 8, 954–973.
Poppe, L., Rué, L., Robberecht, W., and Van Den Bosch, L. (2014). Translating biological findings into new treatment strategies for amyotrophic lateral sclerosis (ALS). Exp. Neurol. 262, 138–151.
Reggio, A., Rosina, M., Krahmer, N., Palma, A., Petrilli, L.L., Maiolatesi, G., Massacci, G., Salvatori, I., Valle, C., Testa, S., et al. (2020). Metabolic reprogramming of fibro/adipogenic progenitors facilitates muscle regeneration. Life Sci. Alliance 3.
Salvatori, I., Valle, C., Ferri, A., and Carrì, M.T. (2017). SIRT3 and mitochondrial metabolism in neurodegenerative diseases. Neurochem. Int. 109, 184–192.
Salvatori, I., Ferri, A., Scaricamazza, S., Giovannelli, I., Serrano, A., Rossi, S., D'Ambrosi, N., Cozzolino, M., Giulio, A. Di, Moreno, S., et al. (2018). Differential toxicity of TAR DNA-binding protein 43 isoforms depends on their submitochondrial localization in neuronal cells. J. Neurochem. 146, 585–597.

TABLE S1. Target genes and oligonucleotide sequences, Related to Figure 2, Figure 5, Figure 6, Figure 8, Figure S2, Figure S5.

Target	Forward sequence	Reverse sequence
TNF-alpha	5'-CTGTGAAGGGAATGGGTGTT-3'	3'-CCCAGCATCTTGTGTTTCTG-5'
IL2	5'TAGGCCACAGAATTGAAAGATCT-3'	3'-GTAGGTGGAAATTCTAGCATCATCC-5'
ND3	5'-CCCTTACGAGTGCGGCTTC-3'	3'-AGTGGCAGGTTAGTTGTTTGTAGG-5'
ND5	5'-AGCATTCGGAAGCATCTTTG-3'	3'-TCGGATGTCTTGTTCGTCTG-5'
COX3	5'-CACTAAATCAAGCCCTACTA-3'	3'-GAAATGGAGAATGATGTTTCA-5'
MyHCI	5'-TGCAGCAGTTCTTCAACCAC-3'	3'-TCGAGGCTTCTGGAAGTTGT-5'
MyHCIIa	5'-AGTCCCAGGTCAACAAGCTG-3'	3'-GCATGACCAAAGGTTTCACA-5'
MyHCIIx/d	5'-AGTCCCAGGTCAACAAGCTG-3'	3'-CACATTTGGCTCATCTCTTGG-5'
MyHCIIb	5'-AGTCCCAGGTCAACAAGCTG-3'	3'-TTTCTCCTGTCACCTCTCAACA-5'
Pgc1α	5'-GTCAACAGCAAAAGCCACAA-3'	3'-TCTGGGGTCAGAGGAAGAGA-5'
Glut-4	5'-GGCATGGGTTTCCAGTATGT-3'	3'-GCCCCTCAGTCATTCTCATG-5'
Nor1	5'-TACGCCACGCAGACTTATGG-3'	3'-TGGTCAGCTTGGTGTAGTCG-5'
Pdk4	5'-AAAGAGGCGGTCAGTAATCC-3'	3'-TCCTTCCACACCTTCACCACA-5'
Serca1	5'-CACCACCAACCAGATGTCAG-3'	3'-TCAAGACCTCTCCCTCAGGA-5'
Serca2a	5'-TCTCCTTGCCTGTGATCCTC-3'	3'-GCACCCGAACACCCTTATATT-5'
Serca2b	5'-AGTTGAGCCAGCAGACATTG-3'	3'-CCAGAGAATCATGCAAAAGACA-5'
Phospholamban (Pln)	5'-CACGTCAGAATCTCCAGAACC-3'	3'-GCTCTTCACAGAAGCATCACA-5'
Myoregulin (Mln)	5'-CAACGTTGCTAGGAGAACAC-3'	3'-GCTCTTGCCACTCATGTTCA-5'

Sarcolipin (Sln)	5’-TGAGGTCCTTGGTAGCCTGA-3’	3’-CACACCAAGGCTTGTCTTCA-5’
AchRα	5’-GGCTTTCACTCTCCGCTGAT-3’	3-’TCAGCGGCGTTATTGGACTC-5’
AchRε	5’-CTCTGCCAGAACCTGGGTG-3’	3’-GACAGTTCCTCTCCAGTGGC-5’
Nav1.5	5’-AGATGTCTCCCCCAGTAACCA-3’	3’-CTTGGGGAGCCTGTCTCTC-5’
Hdac4	5’-TGTACGACGCCAAAGATGAC-3’	3’-CGGTTCAGAAGCTGTTTTCC-5’
Myogenin	5’-TCAGACAGGGTCCATCCCAT-3’	3’-GCTGACTGTGAGCATCCACT-5’
MuRF-1	5’-GACAGTCGCATTTCAAAGCA-3’	3’-AACGACCTCCAGACATGGAC-5’
Myostatin	5’-CTGTAACCTTCCCAGGACCA-3’	3’-TCTTTTGGGTGCGATAATCC-5’
Myoglobin	5’-CTGTTTAAGACTCACCCTGAGAC-3’	5’-GGTGCAACCATGCTTCTTCA-3’
TATA box binding protein	5’-CCAATGACTCCTATGACCCCTA-3’	3’-CAGCCAAGATTCACGGTAGAT-5’